Journal of Hydrology 574 (2019) 1020–1028

Contents lists available at ScienceDirect

Journal of Hydrology

journal homepage: www.elsevier.com/locate/jhydrol

Research papers

Optimal experimental design for calibration of a new sewer water quality model

Julia M. Ledergerber[a,b,*], Thibaud Maruéjouls[c], Peter A. Vanrolleghem[a,b]

[a] modelEAU, Département de génie civil et de génie des eaux, 1065, avenue de la Médecine, Université Laval, Québec, QC G1V 0A6, Canada
[b] CentrEau, 1065, avenue de la Médecine, Université Laval, Québec, QC G1V 0A6, Canada
[c] Le LyRE, Suez Eau France SAS, Domaine du Haut-Carré 43, rue Pierre Noailles, 33400 Talence, France

ARTICLE INFO

Keywords:
Efficient data collection
Model-based planning
Sewer sediments
Measurement campaign

ABSTRACT

Water quality data in the sewer system are indispensable for modelling, but rarely available, as measurements in sewers are challenging to conduct. Optimal experimental design (OED) is a powerful tool to identify and maximize the information content of measurement data. This paper adopts a model-based OED methodology to efficiently plan a measurement campaign for final model calibration and validation of a new sewer water quality model. To do so, a preliminary calibrated model of the case study is used to evaluate the information content of different potential measurement locations and scenarios for suspended solids as measured variable. The case study first demonstrates how OED can identify the best measurement location within a complex sewer network. It secondly demonstrates that measuring the beginning of a big rain event results in the most information-rich data among all scenarios evaluated. Thirdly, it analyses in detail the information content of dry weather flow (DWF) data. In comparison to previous studies the methodology is improved by considering the actual measurement error characteristics when calculating the information content of measurement data.

1. Introduction

Tackling the question of total suspended solids (TSS) in sewer systems goes beyond simply understanding the fate of particulates throughout the sewer system itself. TSS is known as a carrier of nutrients, but also as a carrier of heavy metals, pesticides and pathogens among others; moreover, it is the cause of organic and inorganic pollution. TSS can thus be considered an indicator substance (Vanrolleghem et al., 2018). Developing models for the prediction of the TSS flux for the control of overflow structures or the optimal management of the wastewater resource recovery facility (WRRF) has therefore far-reaching benefits.

Water quality modelling for particulates remains challenging in the sewer. A main reason are the complex processes involved when it comes to TSS, as they greatly transcend mere advective transport. Particles can settle and resuspend; depending on the condition, they can flocculate, aggregate or break; and once settled, they can be consolidated on the bottom of the sewer pipes. In addition, different physical, chemical and biological processes take place both in the water phase and the sewer sediments (Ashley et al., 2004). Modelling developments are on-going, focusing on one or several processes to improve the understanding of those specific processes (e.g. for gross solids, Penn et al., 2018, or for bed load, Mohtar et al., 2018). But even if models are currently not able to incorporate all the processes involved, they help to understand the behaviour of TSS in sewer systems.

Independent of the TSS process modelled, data are indispensable for model calibration and validation. In particular, calibrating dynamic models benefits from high-resolution data as provided by online sensors. Unfortunately, these data are rarely available, as measuring in the sewer system is not very widespread and ambitious to conduct. Furthermore, they are distributed systems that may require measurements at multiple locations (Vanrolleghem et al., 1999). Measurements in sewers not only require a considerable investment in the equipment and the set-up of the measurement site, but also require a tight and intensive maintenance schedule to ensure measurements of reliable quality. The sensors need to be manually cleaned, calibrated and validated, which includes labour-intensive laboratory experiments (Ledergerber et al., 2017).

Moreover, not all data have the same information content for model calibration and validation. In order to calibrate a parameter, the parameter has to be influential during the time period when the data are collected (Dochain and Vanrolleghem, 2001). If a data set is

* Corresponding author at: modelEAU, Département de génie civil et de génie des eaux, 1065, avenue de la Médecine, Université Laval, Québec, QC G1V 0A6, Canada.
E-mail address: julia-margrit.ledergerber.1@ulaval.ca (J.M. Ledergerber).

https://doi.org/10.1016/j.jhydrol.2019.05.004

Available online 04 May 2019

available for calibration and validation of a complex model where overparameterization might be an issue, identifiability analysis is a method to assess the parameters that can be estimated from the given measurement data set (Freni et al., 2011). If, however, a new data set is to be collected, model-based optimal experimental design (OED) can evaluate prior to the measurement campaign which potential experiment of a set of proposed experiments contains the most information for model calibration (Vanrolleghem et al., 1995). OED has mostly been applied in laboratory scale experiments and therefore in a controlled environment (see for example Vanrolleghem and Coen, 1995). OED utilizes a preliminary model that has been calibrated on an initial set of data: first, different experiments are proposed and simulated with the preliminary model; then simulation results are evaluated in terms of their information content (De Pauw and Vanrolleghem, 2006a). The information content of an experiment can be calculated from the Fisher Information Matrix (FIM), indicated in Eq. (1):

$$\mathrm{FIM} = \sum_{k=1}^{N} \left(\frac{\partial y_i}{\partial \theta_j}(t_k) \right)^T Q(t_k) \left(\frac{\partial y_i}{\partial \theta_j}(t_k) \right) \quad (1)$$

The FIM links the information content of an experiment to the sensitivity of the model output corresponding to the measurements y_i with respect to the parameters studied θ_j for the timesteps t_k during the period of the experiment (time step 1 to N) and a square matrix $Q(t_k)$ with user-supplied weighting coefficients (De Pauw and Vanrolleghem, 2006a). $Q(t_k)$ is typically chosen as the inverse of the measurement error covariance or as the identity matrix (Vanrolleghem et al., 1995). An important characteristic of the FIM is the fact that the inverse of the FIM corresponds to the parameter estimation error covariance matrix V (Dochain and Vanrolleghem, 2001), thus allowing the direct assessment of the confidence region of the calibrated parameters. Different criteria exist to evaluate the information content of the proposed experiments, see for example Mehra (1974).

This paper transcends the laboratory scale use of OED by applying it to design a measurement campaign in a full-scale sewer environment. It studies how the potential information content of a new measurement data set can be optimized. It starts from the point that a first measurement campaign has already been conducted without OED. This allows calibrating and validating a preliminary model and approximating the measurement error. A preliminary model is required for planning the second measurement campaign with OED in the most efficient way, making optimal use of the investments, such as measurement equipment and working hours for maintenance. In addition, the results of the first measurement campaign permit approximating the measurement error for the weighting coefficients of the square matrix $Q(t_k)$, rather than working with the identity matrix assumption as previous studies (Vanrolleghem et al., 1995; Freni and Mannina, 2012).

This paper illustrates how OED can be adopted considering an approximation of the measurement error to select the best location for measurements and to the best timing of the measurement scenarios. In the end a more detailed analysis of the experiments performed under dry weather flow (DWF) conditions highlight the importance of considering the measurement error.

2. Material and methods

2.1. Case study

2.1.1. Description

The studied sewer system of the WRRF “Clos de Hilde” (CdH) is located in the southern parts of Bordeaux, France. The WRRF has a treatment capacity of approximately 400 000 PE and the catchment covers about 8 000 ha. The catchment is shown in Fig. 1 and is located on both sides of the river Garonne, which is the main receiving water. The sewer system consists of both combined and separate sewers. For more details, see Ledergerber et al. (2017). Local regulations for the WRRF include TSS, COD and BOD_5 concentrations thresholds at the effluent (JORF, 2015). And importantly, this recent decree (JORF, 2015) sets for the first time combined sewer overflow (CSO) water quality standards that cities will have to apply in the near future.

2.1.2. Available data and models

Data regarding water quantity (flow) are available throughout the sewer system and provided by the local utility. Several continuous flow measurements exist, mainly at pumping stations. In addition, a calibrated hydraulic model, implemented in Mike Urban (DHI, Denmark), is available for the studied catchment.

Water quality data is generally collected by the utility only at the WRRF. In the framework of this project, a first measurement campaign to obtain an initial data set for water quality in the sewer system was conducted in 2017.

2.1.3. Measurement equipment and installation

Two Automatic Measurement Stations (AMS; RSM30, Primodal Systems, Hamilton ON, Canada) are available on site (Rieger and Vanrolleghem, 2008). Both are equipped with two TSS sensors based on different measurement principles. One sensor is a turbidity meter (ViSoTurb 700 IQ, WTW, Weilheim, Germany), which measures the intensity of light scattered at 90 degrees as a beam of light passes through a water sample. The second sensor is a spectrometer (spectro::lyser, s::can Messtechnik, Vienna, Austria), measuring absorption spectra in the UV/vis range. The sensors are calibrated and validated with laboratory TSS samples. To collect the data for the preliminary model during the first measurement campaign, one AMS was installed at the inlet of the WRRF CdH, while the other AMS was installed at the major pumping chamber Noutary (NT). The location of the sensors is indicated in Fig. 1. For more details on the installation at the measurement sites, see Ledergerber et al. (2017). The data quality of the measurements was assured by applying a univariate data quality assessment method (Alferes et al., 2013) resulting in validated high frequency data (minimum one value per three minutes).

2.2. Preliminary model

2.2.1. Modelling approach and software

The preliminary model, with which the OED is applied, includes the catchments and the sewer network of the WRRF CdH.

The catchment model used is the KOSIM-WEST model with the extensions proposed by Pieper (2017). It includes sub-models for flow and pollution generation during wet weather flow (WWF) on the one hand and DWF on the other hand. The two main extensions regard firstly the possibility of routing DWF with linear reservoirs in series and secondly the splitting of the WWF in two parallel sets of linear reservoirs, which allows the user to capture the varying dynamics, especially in the context of larger, aggregated models (Pieper, 2017).

The sewer model uses the so-called particle settling velocity distribution (PSVD) linear reservoirs in series model (Maruéjouls et al., 2015). From a hydraulic perspective, it is a comparably simple modelling approach, but allows considering advective transport, settling and resuspension of ten different particle classes keeping the computational time very competitive. The distribution of settling characteristics of a TSS sample can be measured with the ViCAs experiment, resulting in the PSVD curve of a sample (Chebbo and Gromaire, 2009). Based on these measurements the total TSS is fractionated into the ten classes of the sewer model. The particles of a certain class settle with the settling velocity characteristic of their class. The resuspension rate r_{resusp} (d^{-1}) is calculated using sigmoidal Eq. (2), where Q_{In} (m^3/d) is the inflow of the linear reservoir; $r_{resusp,max}$ (d^{-1}) corresponds to the maximum resuspension rate reached for big inflows; Q_{half} (m^3/d) represents the inflow at which half of the resuspension rate is reached and n (−) is the exponent defining steepness of the sigmoidal curve. The parameters $r_{resusp,max}$, Q_{half} and n have to be calibrated for each sewer

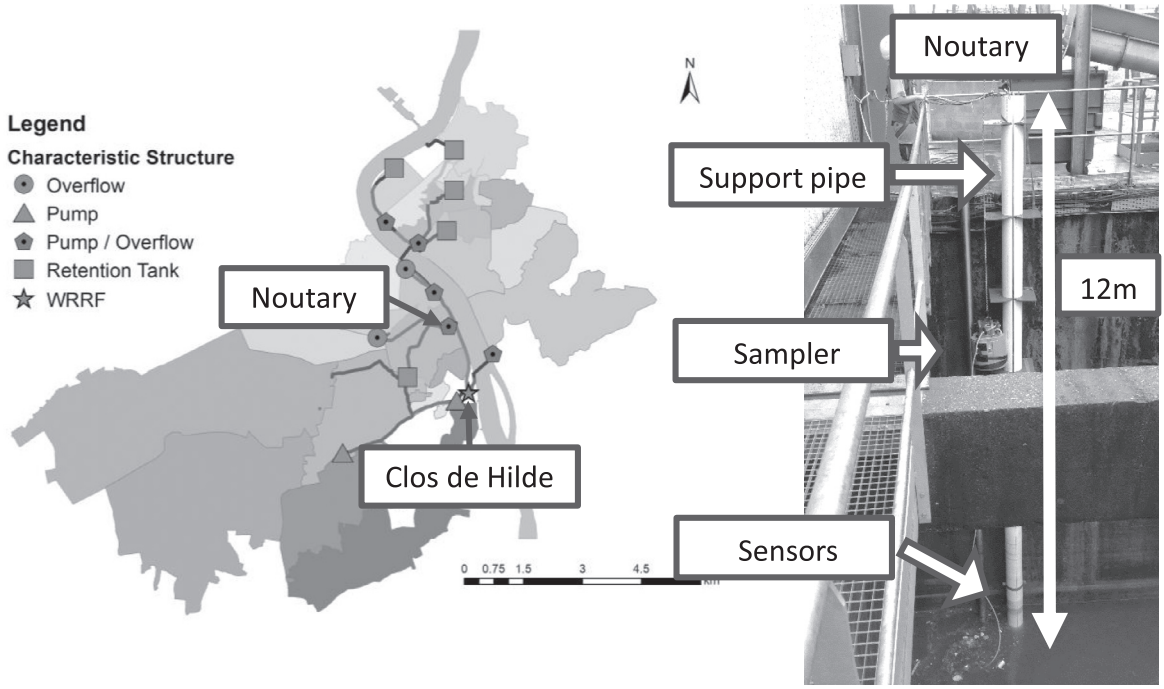

Fig. 1. Catchment and Sensor Installation. Catchment of the WRRF Clos de Hilde (left side) with an illustration of the installation of the AMS at the measurement site Noutary (right side).

stretch. The model is implemented in the software WEST by DHI (Horsholm, DK).

$$r_{\text{resusp}}(t) = r_{\text{resusp,max}} \frac{Q_{\text{In}}^{n}(t)}{Q_{\text{In}}^{n}(t) + Q_{\text{half}}^{n}} \quad (2)$$

2.2.2. Calibration and validation of preliminary model

The preliminary model for OED was calibrated for water quantity (flow) and water quality (TSS). The water quantity model for WWF was calibrated and validated (RMSE = 0.058 m^3/s) on the existing calibrated Mike Urban by DHI model. Only the DWF parameters had to be recalibrated on actual flow measurements, as the Mike Urban model focused on WWF. The validation period on actual flow measurements during a 4-day period, including WWF, is indicated in Fig. 2 (left-hand side) and resulted in a RMSE of 0.064 m^3/s.

The preliminary water quality calibration and validation was conducted using validated TSS data obtained during the first measurement campaign. The time series were chosen based on an analysis of quality of the available data. A coherent measurement set was selected in which high quality data from both AMS were available at the same time. The model was calibrated on a 10-day period including two rain events and was validated for the same 4-day period as the data set used for water quantity model validation, also indicated in Fig. 2. Validation resulted in a RMSE of 58 mg TSS/l.

2.3. OED methodology

2.3.1. Overview of methodology

As mentioned in the previous Section 1, the core of OED is the calculation of the FIM and the evaluation of the experiments for a specific criterion. However, OED has to be viewed in a broader context. Fig. 3 shows the OED methodology applied for this case study. It was inspired by many previous studies (e.g. De Pauw and Vanrolleghem, 2006a; Vanrolleghem and Coen, 1995; Vanrolleghem et al., 1995). The methodology is divided into two phases: the preparation phase (left) and the actual experimental design phase (right).

2.3.2. Preparation phase

The intended outcome of the preparation phase is a preliminary model, with which (a) future planned experiments can be evaluated, (b) the measurement error can be characterized, and (c) initial values can be assigned to the set of parameters for which the OED and, ultimately, the measurement campaign is conducted. The preparation phase consists of three steps, the first of which is inherent to all modelling tasks (Dochain and Vanrolleghem, 2001): identifying the purpose of the model and with it the modelling objectives as well as the choice of

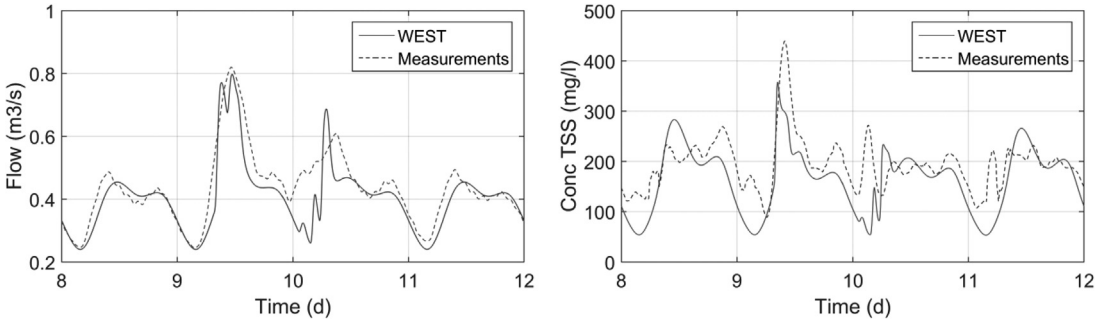

Fig. 2. Model Validation. Validation of preliminary model for water quantity (left-hand side) and water quality (right-hand side).

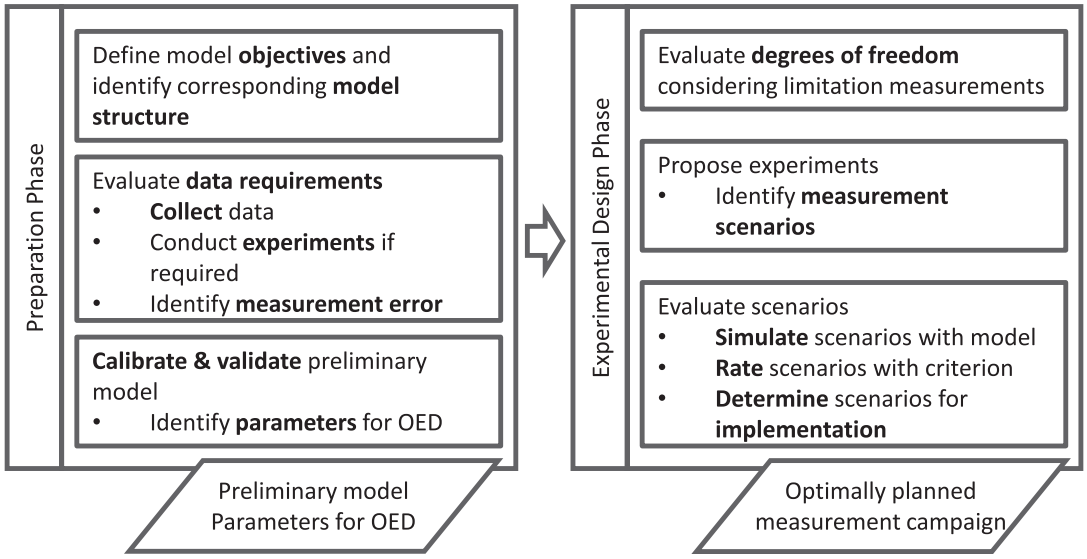

Fig. 3. OED Methodology. Proposed schema for the OED methodology.

corresponding model structure. The second step is to evaluate the data requirements for model calibration and validation. The data for the preliminary model have to be collected, which can include either obtaining available data or conducting a first measurement campaign if not sufficient data are available. An important aspect of this step is to analyse the measurement data and characterize the measurement error. The third step of the preparatory phase is to build, calibrate and validate the preliminary model and identify the parameter set for OED. Manifold references to calibration and validation criteria exist (see for example Hauduc et al., 2015).

2.3.3. Experimental design phase

The output of the second phase, the actual experimental design phase, is the optimally designed measurement campaign in view of recalibration of the identified parameters. This phase consists of three different steps. The first step is to propose experiments that could potentially be conducted. In the context of a sewer system, this step is better described as the identification of the measurement scenarios, as, unlike in laboratory conditions, the measurement conditions as such cannot be influenced, but the timing and location of the measurements can be chosen. The proposed scenarios have to be realistic with respect to the available measurement equipment, the duration of the campaign and the work required for implementation of the experiment. The second step is then to evaluate the proposed scenarios in terms of expected information content, taking the proper measurement error into account. Given the results of the OED evaluation criteria for the different scenarios proposed, the accordingly optimized measurement campaign can be implemented.

2.4. Additional information calculation

2.4.1. Considered parameters for OED

The overall aim of the OED for this model is to improve TSS predictions at the WRRF and, during WWF, also at CSOs. As water quantity parameters are constrained by the water balance and were felt to be already well calibrated on the basis of the Mike Urban model, only the parameters for water quality were considered for OED. The 29 parameters affecting water quality are present both in the catchment and the sewer sub-model. The parameters to be recalibrated are the following parameters: (i) in the catchment sub-model, the mean concentrations under DWF, WWF and infiltration flow, and (ii) in the sewer sub-model, the re-suspension parameters in each of the series of linear reservoirs ($r_{resusp,max}$, Q_{half} and n). As the particle setting velocity distributions were obtained from good quality laboratory ViCAs experiments, they were not considered as parameters to be included in the design of the second measurement campaign. Also, in contrast to other OED studies, e.g. Vanrolleghem et al. (1995), the initial conditions of all state variables of the model were not part of the OED. Indeed, they were not relevant for the simulation results as several days of warm-up were used in the simulations before the actual scenarios were simulated.

2.4.2. Calculation of parameter sensitivity

To complete the Fisher Information Matrix elements, the local sensitivity was calculated at each anticipated measurement point for the second measurement campaign as the central difference, according to Eq. (3) (De Pauw and Vanrolleghem, 2006b). The perturbation factor $\Delta\theta_j$ to calculate the sensitivity was $+/-$ 1% of the parameter value for each of the parameters θ_j.

$$\frac{\partial y_i}{\partial \theta_j}(t) \approx \frac{y_i(t, \theta_j + \Delta\theta_j) - y_i(t, \theta_j - \Delta\theta_j)}{2\Delta\theta_j} \quad (3)$$

2.4.3. Definition of measurement error of TSS

As indicated in Section 2.1.3 the data obtained in the first measurement campaign of 2017 was filtered using the method developed by Alferes et al. (2013). The comparison of the raw and the filtered data allows characterizing the measurement error $|\varepsilon|_{meas,TSS}$, which is defined as the absolute difference of the filtered ($data_{filtered}$) and the raw data ($data_{raw}$), as in Eq. (4):

$$|\varepsilon|_{meas,TSS}(t) = |data_{filtered}(t) - data_{raw}(t)| \quad (4)$$

2.4.4. Evaluation criterion for OED

For this study the D-optimal design criterion in Eq. (5) is chosen among the available scalars that can be calculated from the FIM (Mehra, 1974). As the FIM is the inverse of the parameter estimation error covariance matrix, maximising the determinant of the FIM results in minimizing the volume of the covariance matrix, thus minimizing the parameter estimation error (Dochain and Vanrolleghem, 2001).

$$\max[\det(FIM)] \quad (5)$$

3. Results

First, some general information about the results is presented in Section 3.1. In the following Section 3.2 the optimal location of the

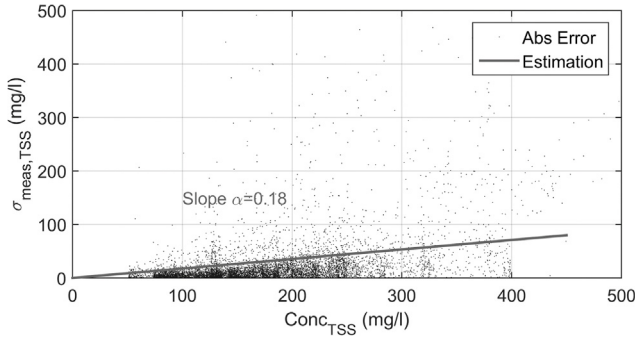

Fig. 4. Measurement Error. Linear dependency of absolute measurement error $|\varepsilon|_{meas,TSS}$ on TSS concentration at pumping station NT.

AMS is evaluated and then in Section 3.3 different scenarios for the chosen optimal location are studied. In the final Section 3.4 DWF measurements are studied in more detail.

3.1. General results

3.1.1. Measurement error estimation of TSS

Based on the assumption that the relative measurement error α does not depend on the TSS concentration ($Conc_{TSS}$), the absolute measurement error ($|\varepsilon|_{meas,TSS}$), as defined in Section 2.4.3, depends linearly on $Conc_{TSS}$:

$$|\varepsilon|_{meas,TSS} = \alpha * Conc_{TSS} \quad (6)$$

This relationship can be observed in Fig. 4 for the TSS measurements at the pumping station NT.

The coefficient α was obtained by fitting the above equation using least squares regression for both measurement locations: 0.09 for the inlet of the WRRF CdH and 0.18 for the pumping station NT. This difference between locations confirms the experience of the far more challenging measurement conditions in the sewer than at the WRRF.

3.1.2. Degrees of freedom and constraints for OED

In order to be able to identify the best possible experiments, hereafter named scenarios for the reasons mentioned in Section 2.3.3, the degrees of freedom of the measurement campaign had to be identified. They include the location of the AMS and thus the location of the measurement set-up as well as the timing of the measurement, differentiating between WWF and DWF and identifying different timings for both situations. Knowledge of the typical performance of the used measurement equipment and anticipation of different measurement conditions allow proposing measurement scenarios.

The experience of the first measurement campaign showed that maintenance of the sensors is of fundamental importance and that sensors give only reliable data for a relatively short period of time after a maintenance event (Ledergerber et al., 2017). For the given case study, it is assumed that, in the worst case, the reliable period lasts for only about 12 h after a maintenance event. So, scenarios of 12 h were planned with a measurement interval of three minutes, corresponding to the storage interval for the online sensors.

Different measurement scenarios were then created for the typical DWF pattern. For DWF, the day is split into day and night conditions, splitting at 09:30, respectively 21:30, assuming that a workday starts at 09:00 at the site and sensors would have received their routine maintenance and be ready for use by 09:30. Measurement scenarios were also defined for WWF conditions, considering that, in contrast to DWF conditions, each rain event is different. To have representative rain scenarios, the proposed experiments were simulated using actual rain data of the previous measurement campaign, conducted in 2017. One big summer storm (cumulative 24 h rainfall: 24.9 mm) was chosen in which multiple overflows were taking place in addition to a smaller rain event (cumulative 24 h rainfall: 2.4 mm). Similar rains were observed several times over the summer of 2017. In total seven different scenarios were proposed, summarized in Table 1.

Table 1
Description of scenarios and resulting values of the D-optimal criterion for chosen AMS location (NT and CdH).

#	Description scenario	Characteristics	D-Opt value
1	Day long DWF period	Preceding DWF: 7 days	5.7E−142
2	Night long DWF period	Preceding DWF: 7 days	4.2E−127
3	Day following WWF	Preceding DWF: 0 days	2.6E−136
4	Night following WWF	Preceding DWF: 0 days	3.0E−127
5	Entire small rain event	24 h cumulative rain: 2.4 mm	3.9E−115
6	Beginning big rain event	24 h cumulative rain: 24.9 mm	9.0E−91
7	Tail big rain event	24 h cumulative rain: 24.9 mm	2.7E−117

3.2. OED for evaluation of measurement location

For the planned measurement campaign, the OED methodology was used to re-evaluate the original location of the AMS at NT and CdH with respect to the information content of the measurement data. As mentioned initially, two AMS were available for the measurement campaigns. During the first measurement campaign in 2017, which was designed based on expertise and practical experience, one AMS was installed at the inlet of the WRRF CdH and the second was placed at the pumping station NT in the sewer system. The location of the AMS in the sewer system was re-evaluated, using seven other locations as possible locations (see Fig. 5). The evaluated locations correspond all to pumping stations or retention tanks upstream of the WRRF in the sewer system. The first AMS was always maintained at the inlet of the WRRF since this is the final outlet of the sewer system. As preliminary measurements were only available at the pumping station NT and the inlet of the WRRF CdH, the measurement error could only be estimated for those two locations. For the OED calculations, it was assumed that the measurement error found at NT was representative of the other seven locations in the sewer system.

For the evaluation of the location of the AMS, timing scenario 6 (beginning of big rain event) was chosen, as this was expected to be the best scenario independent of the location chosen, given the large TSS dynamics occurring (this will be confirmed in Section 3.3). Fig. 6 illustrates how the value of the D-optimal criterion changes according to the location of the AMS (for timing scenario 6). The location of the AMS at the pumping station NT chosen for the first measurement campaign ranks third among the eight identified options. The two places that rank better are located further upstream and contain information about the sewer system on the right bank of the Garonne, which NT lacks.

For the second measurement campaign a re-location of the AMS from NT to either CV&JR or JR was therefore considered. A closer evaluation of the sites, however, revealed that those locations were not practical, either due to the elevated risk of vandalism (JR) or accessibility (CV&JR). The location of the AMS for the second measurement therefore remained at NT as it was the best possible location of those that were practically feasible.

3.3. OED for evaluation of measurement scenarios

Having both location and timing as degrees of freedom (see Section 3.1.2) results in a two-dimensional problem, as the evaluation of the timing scenarios depends on the location of the AMS chosen. Therefore, it was first analysed how often a timing scenario is evaluated as the most information-rich scenario for all possible measurement locations before analysing the results in more detail for the chosen location of the AMS. In the last step the influence of the distance from the measurement point to the series of linear reservoirs on the identifiability of their respective local parameters was studied.

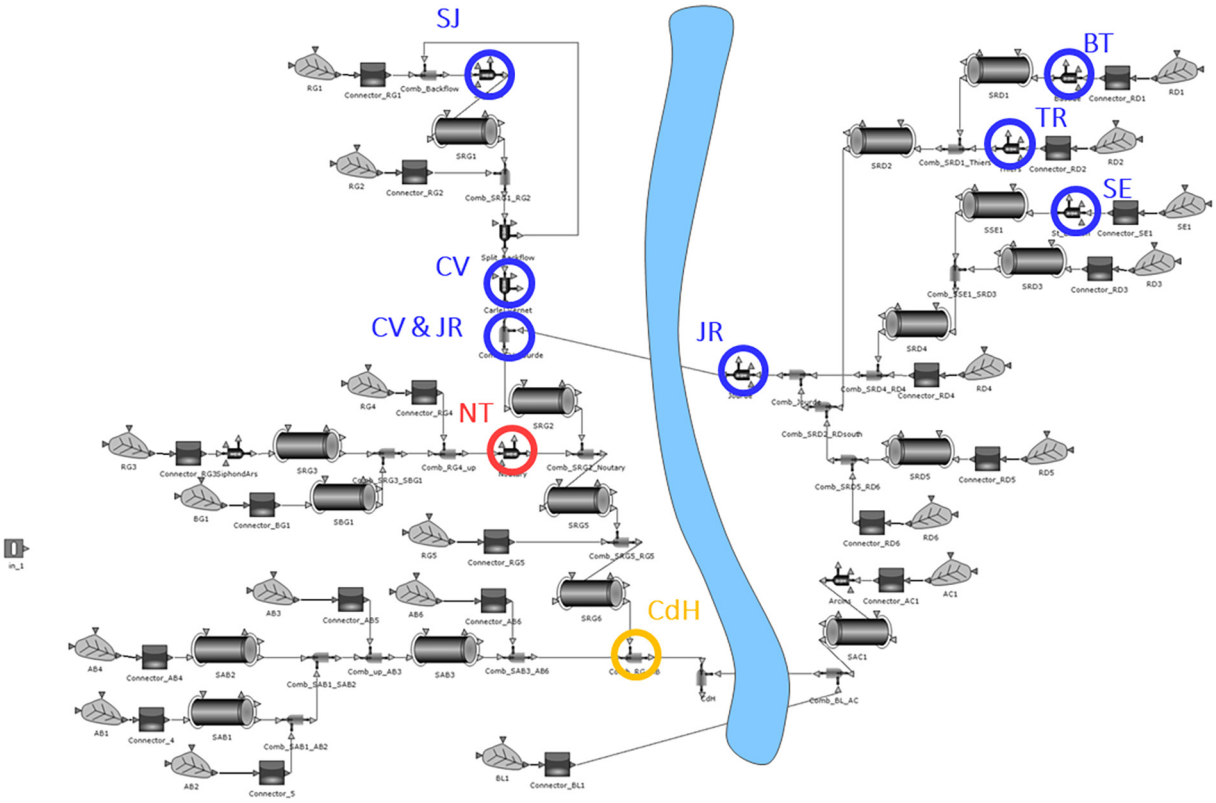

Fig. 5. Potential AMS Locations. Schema of the "Clos de Hilde" catchment with eight different identified locations of AMS.

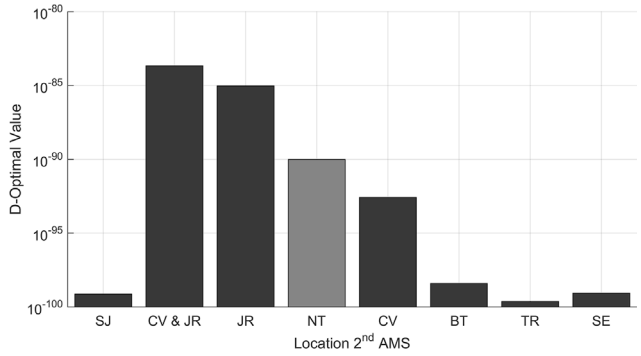

Fig. 6. Comparison AMS Locations. Information content for different locations of the second AMS in the sewer (for timing scenario 6).

3.3.1. Most Information-rich scenario

Fig. 7 shows for how many locations a timing scenario was the most information-rich among the eight different locations. The analysis was conducted once for all DWF and WWF scenarios and once for the DWF scenarios only (scenario 1–4). The results show that, independent of the location chosen, the best-case scenario is always scenario 6, which corresponds to the beginning of a big rain event. If the analysis is conducted for the DWF scenarios only, the results show that in seven out of the eight possible locations, scenario 4 (Night following WWF) contains the most-information rich data. The actual information content (value of the D-optimal criterion) depends on the location and is analysed in detail for the chosen location of the AMS in the next Section 3.3.2.

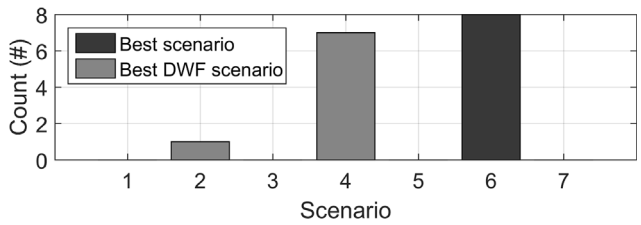

Fig. 7. Evaluation Best Scenario. Number of location pairs for which the given scenario provided the most information content among all scenarios or all DWF scenarios.

3.3.2. Detailed analysis for chosen location

As concluded in Section 3.2, the best practically feasible locations of the two available AMS is the combination of NT and CdH, for which the D-criterion results are summarized in Table 1. One will notice that the absolute values for the D-criterion are very low in absolute terms, but this is due to the units used for the variables and parameters of the model. Optimality of the experiment does not depend on the absolute values, but on the ranking of the D-values.

For the DWF scenarios, only 28 parameters were considered, as the WWF TSS runoff concentration can only be estimated during WWF scenarios. The tabulated results show that the values of the D-criterion are by orders of magnitude higher for the WWF scenarios than for the DWF scenarios. The measurement campaign has therefore to focus on capturing wet weather conditions. It is also to be noted that the beginning of a big rain event is by far richer in information than the tail of the event. In case of DWF-only conditions, the results show that data collected during night (21:30–09:30) are richer in information content than during day (09:30–21:30).

As the inverse of the FIM, V, corresponds to the parameter estimation error covariance matrix, the relative parameter estimation error of each parameter can be evaluated (the squared parameter estimation errors of the parameters j, σ_j^2, are the diagonal elements of the matrix V). The resulting relative parameter estimation error (σ_j/θ_j) is shown for three timing scenarios in Fig. 8, the worst-case scenario 1 (top), the best-case DWF scenario 2 (middle) and the overall best-case scenario 6. The figure clearly shows that parameter identification with only DWF

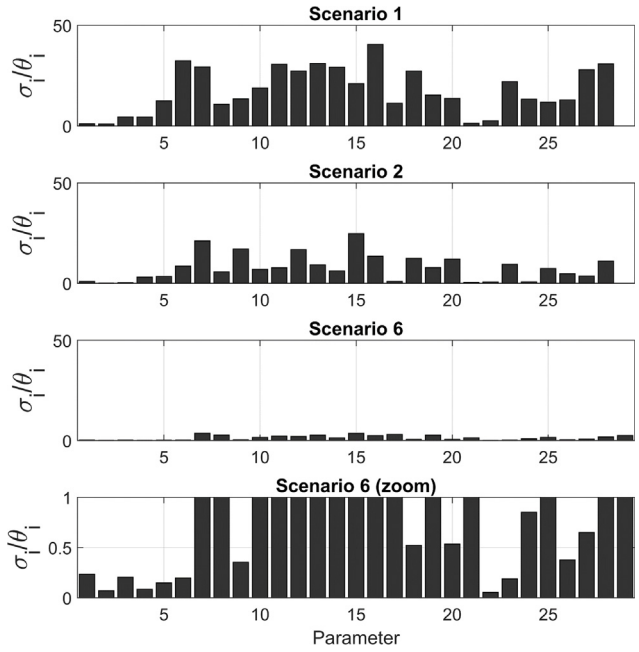

Fig. 8. Relative Parameter Estimation Error. Relative parameter estimation error for the worst-case scenario 1 (top), the best-case DWF scenario 2 (middle) and the overall best-case scenario 6 (bottom), with a zoom on the errors for the best experiment (scenario 6).

measurements, even under the best conditions, is very difficult. Many parameters remain unidentifiable with a parameter estimation error much larger than the parameter value itself ($\sigma_j/\theta_j \gg 1$). An example for this is parameter 5, the flow at which half of the resuspension rate is reached (Q_{half}) for an upstream series of linear reservoirs. In the information-poorest scenario 1, the parameter has a parameter estimation error approximately 12 times its own value, while in the best-case DWF, this ration is only reduced to approximately 3. Analysing scenario 6 in Fig. 8 shows, on the contrary, that the error on the parameter estimation reduces dramatically for most parameters when measurements are conducted under WWF conditions. For instance, parameters 1–6 can now be estimated with a parameter estimation error that is less than 20% of their respective parameter value, an excellent result for water quality process parameters. It must be accepted though that some parameters remain difficult to identify, which is further studied in the next Section 3.3.3.

3.3.3. Parameter estimation error and distance from the measurement point

For the chosen location of the AMS and the best-case scenario 6, the parameter estimation error is studied with respect to where in the model the parameter occurs, i.e. in which sewer stretch the parameter occurs in the model. The hypothesis analysed here is that the farther the sewer stretch is from a measurement point, the lower the information content relative to the parameter occurring in that stretch is. The distance measure that is adopted here is the number of series of linear reservoirs between the sewer stretch of interest and the closest downstream measurement point. For this the layout of the case study shown in Fig. 5 is schematized in Fig. 9, indicating the distance from a measurement point by levels, which indicate the number of series of linear reservoirs. Global parameters are primarily the different TSS concentrations in the catchments, which determine the global mass balance and are thus considered to be “Level zero” parameters.

In Fig. 10 the distance to the closest downstream measurement point is given for the parameters ordered with respect to their error estimation σ_j/θ_j. This figure shows a marked tendency for the parameter estimation error to increase with the distance to the closest downstream measurement point. Global parameters (Level zero) and parameters

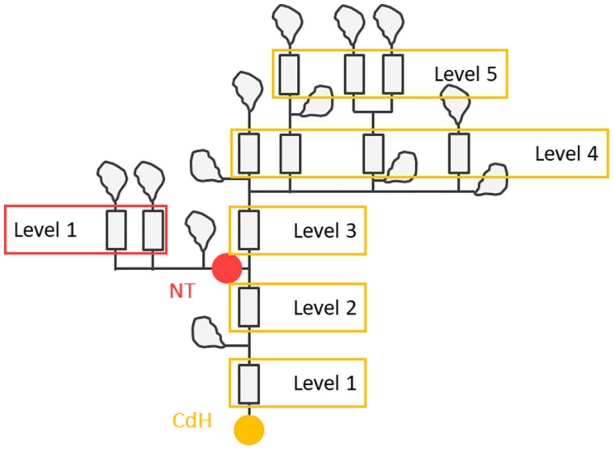

Fig. 9. Definition Distance. Distance from the closest measurement point, indicated as the number of series of linear reservoirs between the measurement point and the sewer stretch in which the parameter of interest occurs.

close to a measurement point can generally be better estimated.

3.4. OED for optimal 12 h measurement segment of DWF day

Following the analysis of the scenarios in the previous section, this last analysis tackles the question of which 12 h segment during stable DWF flow conditions contains the most information. Fig. 11 shows the D-optimal value for every 12 h segment following the full hour of the day. As the previous section already suggested, the information content is highly variable during the day and is lower during measurement segments starting during day hours than during night hours. The 12 h segment with the most information content starts at 02:00.

4. Discussion

In the results Section 3.2, this paper showed how OED can be used to identify the optimal measurement location. The results showed that the chosen location of the measurement station in the sewer, NT, ranked third. The better-ranked locations with regard to information content, CV&JR and JR, were unfortunately not feasible as location of the AMS for practical reasons. This finding about the location of the AMS is consistent with the location of the sewer stretch in which parameters occur that have a large parameter estimation error (see results Section 3.3). It was demonstrated that parameters occurring in sewer stretches located at a large distance to the closest downstream measurement point (high level) are difficult to estimate. In general, those stretches are located on the right bank of the river Garonne. Moving the second AMS to CV&JR or JR would indeed have allowed collecting more information about the parameters in those stretches.

In the results Section 3.3 different measurement scenarios were analysed for the chosen location of the AMS (CdH and NT). It illustrates that for the same effort, i.e. a measurement campaign of 12 h, data of markedly different information content can be obtained depending on the scenario. It was shown that data collected under WWF conditions generally contain more information than those under DWF, with the beginning of a big rain event containing the most information. This is due to the important dynamics occurring during WWF conditions and the first-flush phenomenon observed for the given case study. The scenario analysis for DWF showed that the measurement campaign starting at 21:30 contains more information than the one starting at 9:30. This might be because the TSS concentrations during the night are generally lower than during daytime, which means that the measurement errors are smaller. Thus, the information content per TSS value is higher for the studied parameters.

The results Section 3.4 analysed all theoretically possible 12 h

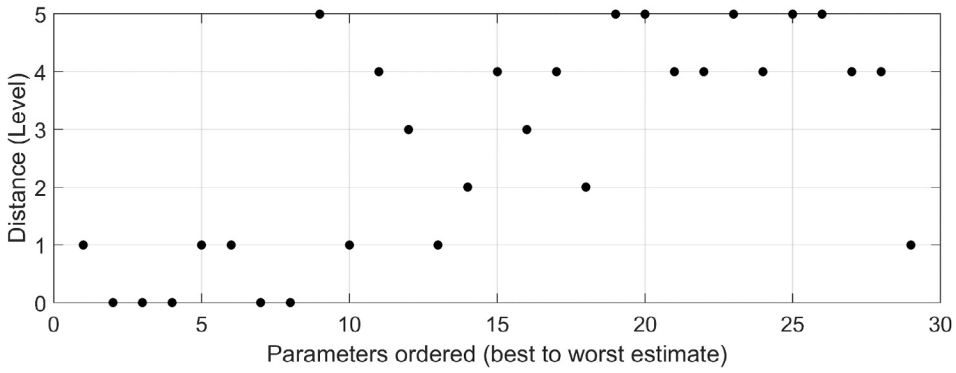

Fig. 10. Parameter Location. Parameters ordered from best to worst parameter error as function of the distance to the closest downstream measurement point.

measurement segments starting at a full hour of a DWF day. Those results confirmed the findings of the previous section and show that the later during a workday the 12 h measurement campaign starts, the more information content the measurement data will have. The analysis also demonstrated that the information content of a measurement segment starting at 02:00 would contain most information, but those segments are not feasible from a practical point of view due to accessibility issues of pumping stations at night.

For the planning of the measurement campaign, it was imposed that the maintenance of the sensors must be performed prior to rain events because, if the sensors fail during a rain event, no maintenance intervention can be conducted for safety reasons. Since the beginning of the rain event is the critically important, this is quite acceptable. In case DWF conditions prevail, the measurement campaign has to start late during the workday, in order to capture the information-rich night values to the fullest extent practicable. Having all of this information allows for planning a measurement campaign in its most efficient way, as it clearly indicates when the measurement campaign should be prepared and started. This ensures the optimal use of the measurement equipment and the limited resources during the campaign.

5. Conclusions

This research demonstrates that adaptation of model-based OED to complex sewer models is possible. It also shows that OED is a valuable tool for planning measurement campaigns in the challenging sewer environment as it allows making optimal use of the investments necessary for such a campaign. In comparison to posterior analysis of a measured data set, OED evaluates the best location and timing for measurements prior to the actual measurement campaign. This would otherwise need to be planned by expert opinion only. OED allows to objectively rank different measurement locations with respect to their information content. This enables balancing how far upstream or downstream an AMS should be placed. With respect to the timing scenarios, both expert opinion and OED identify WWF events as more important than DWF conditions. However, OED also differentiates between the importance of a small versus a big rain event and their beginning versus their tail. From a methodological point of view, it was demonstrated that considering the real measurement error (in this case constant relative error) affects the evaluation of the DWF scenarios. This would not have been possible without the mathematical tools provided by OED.

Declaration of Competing Interest

None.

Acknowledgements

The authors would like to thank two anonymous reviewers for their valuable comments. The authors acknowledge the financial support by a Collaborative Research and Development grant of the Natural Sciences and Engineering Research Council (NSERC) and Suez Treatment Solutions Canada. The authors thank Bordeaux Metropole and Société de Gestion de l'Assainissement de Bordeaux Métropole (SGAC) for technical and financial support. Peter Vanrolleghem holds the Canada Research Chair in Water Quality Modelling.

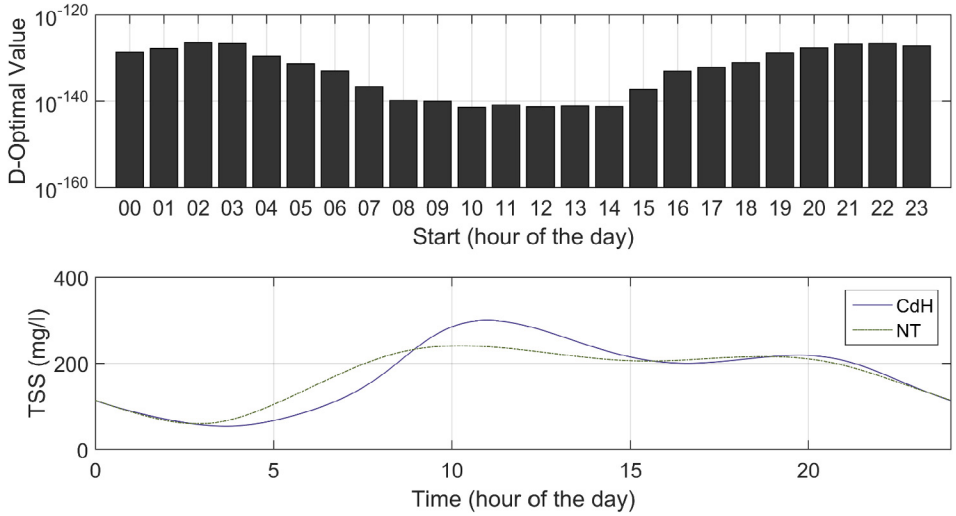

Fig. 11. DWF Evaluation. D-optimal evaluation of the information content of a 12 h measurement campaign, starting at every full hour of the day.

References

Alferes, J., Tik, S., Copp, J., Vanrolleghem, P.A., 2013. Advanced monitoring of water systems using in situ measurement stations: data validation and fault detection. Water Sci. Technol. 68 (5), 1022–1030.

Ashley, R. M., Bertrand-Krajewski, J.-L., Hvitved-Jacobsen, T., and Verbanck, M., 2004. Solids in sewers – Characteristics, effects and control of sewer solids and associated pollutants. IWA Scientific & Technical Report 14, IWA Publishing, London, U.K.

Chebbo, G., Gromaire, M.-C., 2009. VICAS – An operating protocol to measure the distributions of suspended solid settling velocities within urban drainage samples. J. Environ. Eng. 135 (9), 768–775.

De Pauw, D.J.W., Vanrolleghem, P.A., 2006a. Designing and performing experiments for model calibration using an automated iterative procedure. Water Sci. Technol. 53 (1), 117–127.

De Pauw, D.J.W., Vanrolleghem, P.A., 2006b. Practical aspects of sensitivity function approximation for dynamic models. Math. Comput. Modell. Dyn. Syst. 12 (5), 395–414.

Dochain, D. and Vanrolleghem, P. A., 2001. Dynamical Modelling and Estimation in Wastewater Treatment Processes. IWA Publishing, Alliance House, 12 Caxton Street, London SW1H 0QS, UK.

Freni, G., Mannina, G., 2012. The identifiability analysis for setting up measuring campaigns in integrated water quality modelling. Phys. Chem. Earth Parts A/B/C 42, 52–60.

Freni, G., Mannina, G., Viviani, G., 2011. Assessment of the integrated urban water quality model complexity through identifiability analysis. Water Res. 45 (1), 37–50.

Hauduc, H., Neumann, M., Muschalla, D., Gamerith, V., Gillot, S., Vanrolleghem, P.A., 2015. Efficiency criteria for environmental model quality assessment: a review and its application to wastewater treatment. Environ. Model. Softw. 68, 196–204.

JORF, 2015. Arrêté du 21 juillet 2015 relatif aux systèmes d'assainissement collectif et aux installations d'assainissement non collectif, à l'exception des installations d'assainissement non collectif recevant une charge brute de pollution organique inférieure ou égale à 1,2 kg/j de DBO5 (in French). Journal Officiel de la République Française. NOR: DEVL1429608A.

Ledergerber, J. M., Leray, É., Maruéjouls, T., and Vanrolleghem, P. A., 2017. Optimization of installation and maintenance of water quality sensors in combined sewers. In Proceedings of the 14th IWA/IHAR International Conference on Urban Drainage, Prague, Czech Republic, September 10-15 2017.

Maruéjouls, T., Lessard, P., and Vanrolleghem, P. A., 2015. A particle settling velocity-based integrated model for dry and wet weather wastewater quality modeling. In Proceedings of the WEF Collection Systems Conference, Cincinnati, Ohio, United States, April 19-22 2015.

Mehra, R.K., 1974. Optimal input signals for parameter estimation in dynamic systems-survey and new results. IEEE Trans Autom Control 19 (6), 753–768.

Mohtar, W.H.M.W., Afan, H., El-Shafie, A., Bong, C.H.J., Ghani, A.A., 2018. Influence of bed deposit in the prediction of incipient sediment motion in sewers using artificial neural networks. Urban Water J. 15 (4), 296–302.

Penn, R., Schuetze, M., Jens, A., Friedler, E., 2018. Tracking and simulation of gross solids transport in sewers. Urban Water J. 15 (6), 1–8.

Pieper, L., 2017. Development of a Model Simplification Procedure for Integrated Urban Water System Models – Conceptual Catchment and Sewer Modelling. Master's thesis. Université Laval, Québec, QC, Canada.

Rieger, L., Vanrolleghem, P.A., 2008. mon*EAU*: a platform for water quality monitoring networks. Water Sci. Technol. 57 (7), 1079–1086.

Vanrolleghem, P.A., Coen, F., 1995. Optimal design of in-sensor-experiments for on-line modelling of nitrogen removal processes. Water Sci. Technol. 31 (2), 149–160.

Vanrolleghem, P.A., Daele, M.V., Dochain, D., 1995. Practical identifiability of a biokinetic model of activated sludge respiration. Water Res. 29 (11), 2561–2570.

Vanrolleghem, P.A., Schilling, W., Rauch, W., Krebs, P., Aalderink, H., 1999. Setting up measuring campaigns for integrated wastewater modelling. Water Sci. Technol. 39 (4), 257–268.

Vanrolleghem, P. A., Tik, S., and Lessard, P., 2018. Advances in modelling particle transport in urban storm- and wastewater systems. In Proceedings of the 11th International Conference on Urban Drainage, Palermo, Italy, September 23-26 2018.